JOURNAL OF MATERIALS SCIENCE 32 (1997) 4421–4427

Preparation of potassium tantalate niobate through sol–gel processing

C. J. LU*, A. X. KUANG
Department of Physics, Hubei University, Wuhan 430062, People's Republic of China
**and also National Laboratory of Solid State Microstructures and Department of Physics, Nanjing University, Nanjing 210093, People's Republic of China*

Potassium tantalate niobate (KTN) $KTa_{0.65}Nb_{0.35}O_3$ powders and thin films of perovskite structure were prepared through sol–gel processing. A homogeneous and stable precursor solution was obtained from tantalum ethoxide, niobium ethoxide, and potassium ethoxide in absolute ethanol with a key additive of acetic acid. Powder gels were obtained by exposing the solution to atmospheric water, thus hydrolysing the solution. The precursor powder crystallized to pyrochlore at 600 °C, and then completely transformed to perovskite at 750 °C. Alternatively, thin films were deposited on quartz glass, silicon, sapphire, yttria-stablized ZrO_2, $LaAlO_3$, $SrTiO_3$ and platinum-coated silicon plates, using the spinning technique. The crystal structure of the KTN thin films showed a strong dependency on the crystal structure of the substrates. Crack-free and transparent epitaxial KTN thin films were successfully prepared on $SrTiO_3$ (1 0 0) and (1 1 0) substrates and highly oriented KTN films on R-plane sapphire and $LaAlO_3$ (0 1 2) substrates. The chemical composition of the KTN powders and thin films is in good agreement with the atomic ratio of the starting materials.

1. Introduction

Potassium tantalate niobate, $KTa_{1-x}Nb_xO_3$ (KTN), has received a great deal of attention as a ferroelectric material possessing the perovskite structure [1]. Because of its piezoelectric, pyroelectric, and electro-optic properties, the crystal is of interest for application in band filters, infrared detectors, and electo-optic modulators [2–5]. The Curie temperature of KTN can be varied by controlling the Ta : Nb ratio. Key ferroelectric properties are therefore composition-dependent. The highest quadratic electro-optic coefficient was found in the non-ferroelectric cubic phase of KTN ($x = 0.35$) at room temperature [6]. However, the growth of the large KTN crystals is difficult, one of the major problems being the inhomogeneity of the crystal composition [7, 8]. On the other hand, KTN bulk crystals usually exhibit so-called striations [9], which have prevented the wide-spread use of KTN in electro-optic devices. Debely *et al.* [10] reported on the synthesis and electro-optic properties of transparent KTN ceramics prepared from KTN powders above 1200 °C under hot-pressure-sintering conditions. High temperatures are required for the sintering of KTN in order to achieve a truly homogeneous distribution of ions. At the same time, the volatilization of potassium has to be minimized in the conventional solid-state reaction.

Direct thin-film preparation appears, however, much more suitable for electro-optical as well as some other applications, because not only can the bulk-homogeneity problem, the cutting and polishing of thin slabs be avoided, but also these films can afford the possibility for integration with very-large-scale silicon integration technologies. A sol–gel process has been developed for the ferroelectric film fabrication providing several advantages. These advantages include higher purity, lower processing temperatures, good composition control, compositional homogeneity, and versatile shaping. Hirano *et al.* [11] and Nazeri and Kahn [12] demonstrated the synthesis of highly oriented KTN thin films on MgO (1 0 0) substrates and $SrTiO_3$ (1 0 0) and (1 1 0) substrates by the sol–gel method. We have successfully prepared epitaxial KTN thin films on $SrTiO_3$ and these films show excellent electro-optical properties. This paper describes the synthesis of KTN ($x = 0.35$) powders and thin films through metallorganic compounds and the crystallization process of KTN precursor gels and films.

2. Experimental procedure

For solution preparation, tantalum ethoxide, niobium ethoxide, and potassium ethoxide were selected as starting materials and absolute ethanol as the solvent. The handling of chemicals and procedures was conducted in a dry nitrogen chamber. A certain molar ratio of tantalum ethoxide and niobium ethoxide was dissolved in absolute ethanol. Then a stoichiometric ratio of potassium ethoxide, dissolved beforehand in absolute ethanol, was added to the solution and stirred, and reacted again. After concentrating the solution to 0.5 mol l^{-1}, 5 mol % acetic acid was added as a stabilizing agent. The solution, in open glass bottles,

0022–2461

was hydrolysed by the slow absorption of water vapour from the ambient atmosphere. The solution was allowed to polymerize, resulting in an inorganic network composed of metal–oxygen–metal linkages. The stable and partial condensation product was aged for 24 h to form a coating solution.

The final solution was spin-coated at 3000 r.p.m. for 30 s on various substrates in an environment of 20 °C and relative humidity of 50 %, resulting in one-coat, transparent-gel films. Quartz glass, $SrTiO_3$ (1 0 0) and (1 1 0), silicon (1 1 1), platinum-coated silicon (1 1 1), yttria-stabilized ZrO_2 (YSZ) (1 0 0), $LaAlO_3$ (0 1 2), and R-plane sapphire plates were used as substrates. Prior to spin-coating, all substrates were rinsed with deionized water and cleaned in absolute ethanol. The deposited thin films were air-dried for approximately 30 min and then transferred to an air atmosphere quartz-tube furnace for pyrolysis and crystallization. Our TG–DTA results (see Fig. 1) for dried gel were used to determine the heat-treatment parameters. Because large volume change occurs during pyrolysis which may lead to cracks in the films, the thickness of the films had to be built up gradually through successive spin-coating applications in order to reduce the stress developed during the treatment. The intermediate layers were calcined for 30 min at 400 °C and a heating rate of 200 °C h^{-1} was used. Annealing temperature in the range 500–900 °C were specifically investigated to achieve crystalline films. A typical fully crystallized single-layered film had a thickness of approximately 120 nm. The thickness of the film was determined on the fractured cross-section of the substrate by scanning electron microscopy (SEM).

KTN powders were also prepared from the precursor solutions. The solution was hydrolysed by exposure to air in open dishes and allowed to polymerize to form a transparent gel after 1 wk. Gel pieces dried for 1 wk at room temperature were then fired between 500 and 900 °C in air for 3 h.

As-prepared dried gel was analysed by differential thermal analysis (DTA), differential scanning calorimetry (DSC), and thermogravimetric analysis (TG). The prepared powders and films were characterized by X-ray diffraction analysis (XRD) using CuK_α radiation with a monochromator. X-ray photoelectron spectroscopy (XPS) analysis and inductively coupled plasma (ICP) experiments were carried out on these films and powders, respectively, to determine their composition.

3. Results and discussion

3.1. Synthesis of powders

In general, as-prepared dried gels are amorphous and annealing is needed to transform the bulk gel from amorphous structure to the desirable perovskite phase. The amorphous structure will first transform into an intermediate pyrochlore phase and then the pyrochlore phase will transform into perovskite phase at a higher temperature.

Fig. 1 shows DTA and TG curves of the dried KTN gel prepared from the coating solution. Upon heating, a relatively large decrease in weight and a broad endothermic peak observed to about 200 °C is attributed to the evaporation of absorbed water and solvent. Coincidentally, the infrared absorption peaks of O–H (3320 cm^{-1}) and H–O–H (1630 cm^{-1}) bands decreased drastically at this temperature [13]. A large weight loss accompanying an exothermic peak around 320 °C should be due to the drastic removal of acetyl groups and their combustion. Above 320 °C the gel gradually turned to a black colour due to the oxidation of the alkyl groups. On noting that the broad exothermic "peak" from 500–750 °C seems to include several single exothermic peaks, the DSC analysis experiments for the dried gel calcined at 400 °C were carried out, and the results are shown in Fig. 2. It can be seen from Fig. 2 that there are three exothermic peaks at 523.7, 634.5 and 699.5 °C, respectively, in the range 500–750 °C. The powders fired at 650 °C had a white colour and did not show any absorption band assignable to alkyl, and carboxylate groups in the infrared spectrum [13]. The high exothermic peak at 634.5 °C, therefore, accompanies a weight loss which is probably due to the combustion of free carbon; the dried gels were packed into the DSC-TG cell which

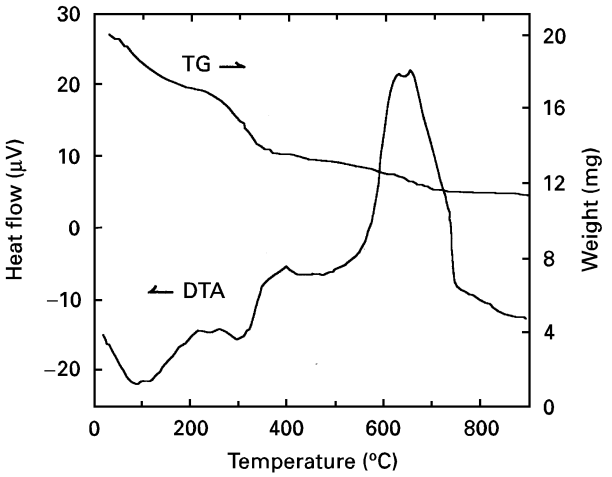

Figure 1 DTA–TG curves of KTN dried gel. The heating rate was 15 °C min^{-1} in air.

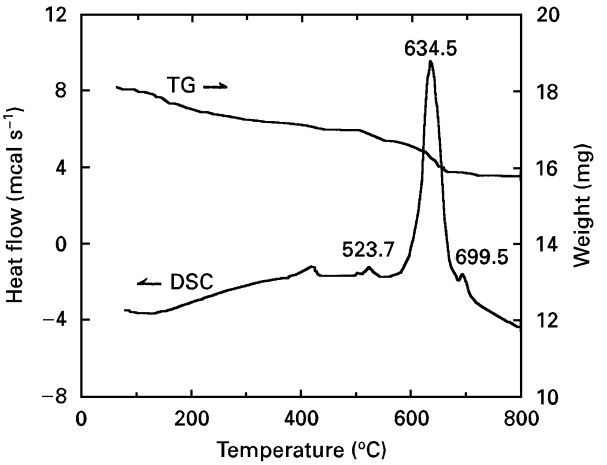

Figure 2 DSC–TG curves of KTN dried gel calcined at 400 °C. The heating rate was 10 °C min^{-1} in air.

leads to the formation of residual carbons. The exothermic peak at 523.7 °C results from the crystallization of pyrochlore phase, and the peak at 699.7 °C is due to the phase transformation from pyrochlore to perovskite, according to our X-ray diffraction analysis.

X-ray diffraction was used to study the phase formation as a function of the annealing temperature [14]. For a firing temperature of 450 °C, no definitive diffraction peak was observed and the powders remained amorphous. Several broad pyrochlore peaks were found at 550 °C. The intensities of the reflections from the pyrochlore structure increase with temperature up to 600 °C, above which they decrease and the perovskite peaks appear. Single-phase KTN powders of a perovskite structure were prepared at or above 750 °C. Fig. 3 illustrates XRD patterns of KTN ($x = 0.35$) powders fired at 600 and 750 °C. The phase identified after treatment at 600 °C matches the JCPD (35-1464) of pyrochlore $K_2Ta_2O_6$. The XRD pattern of KTN powders fired at 750 °C matches the JCPD (38–1470) of perovskite $KTaO_3$. The presence of pyrochlore is commonly recognized when the amorphous KTN films are annealed to form the perovskite phase [11–14]; however, there is little consensus about the exact peak positions and ($h\,k\,l$) identification of the pyrochlore and perovskite structure because no standard polycrystalline powder diffraction file [15] of the KTN pyrochlore or perovskite phase has been established. Table I gives the X-ray diffraction data of $KTa_{0.65}Nb_{0.35}O_3$ perovskite and pyrochlore phase

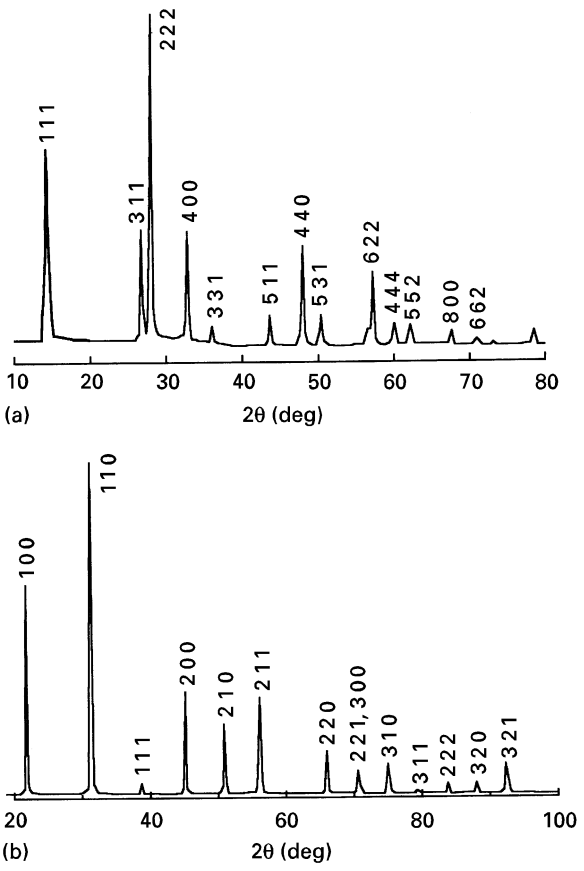

Figure 3 XRD patterns of KTN powders fired at (a) 600 °C and (b) 750 °C.

TABLE I X-ray diffraction data of $KTa_{0.65}Nb_{0.35}O$ perovskite and pyrochlore phase

Pyrochlore			Perovskite		
$h\,k\,l$	d (nm)	I/I_0	$h\,k\,l$	d (nm)	I/I_0
111	0.615	60	100	0.399	61
311	0.320	32	110	0.289	100
222	0.307	100	111	0.230	3
400	0.265	30	200	0.200	32
331	0.244	5	210	0.179	22
511	0.205	9	211	0.163	27
440	0.188	27	220	0.141	13
531	0.180	9	300, 221	0.133	9
622	0.160	21	310	0.128	10
444	0.154	7	311	0.120	2
552	0.149	6	222	0.115	4
800	0.138	4	320	0.111	3
662	0.122	4	321	0.107	10

derived from Fig. 3. The XRD patterns were collected on Rigaku D/max-IIIC X-ray diffractometer. The experimental conditions used were CuK_α radiation, target voltage 40 kV, tube current 25 mA, graphite monochromater, DS/SS 1/2°, RS 0.15 mm, step width 0.01°, and scanning rate 2° min^{-1}. According to the identification results, the lattice constant of perovskite KTN ($x = 0.35$) powders fired at 750 °C is 0.3993 nm.

The atomic ratio of potassium, tanatalum and niobium in KTN powders fired at 750 °C was determined by ICP measurements. The ICP results, 1.00 : 0.67 : 0.34, were in good agreement with the stoichiometry of the starting materials. Actually, no important weight loss was encountered over the annealing range 670–900 °C. These data indicate that there is no tangible loss of any constituent from the powders by evaporation. Infrared absorption spectrum studies were performed to investigate the formation of a complex or double metal alkoxides [14]. The results strongly indicate the existence of a complex reaction resulting in the formation of double metal alkoxides $KNb(OC_2H_5)_6$ and $KTa(OC_2H_5)_6$ in the precursor solution. Complex formation permits homogeneity on the molecular level of the potassium and tantalum and niobium compounds. The high level of homogeneity leads to controllable stoichiometry, a lower reaction temperature and superior electrical properties of sol–gel derived KTN ceramics or thin films, when compared to conventionally processed ceramics or thin films.

3.2. Preparation of thin films

3.2.1. Quartz glass, silicon, and platinum-coated silicon substrates

KTN thin films, with a composition of $x = 0.35$, were prepared on various substrates from the precursor solution by spin-coating. The XRD patterns of films fired at different temperatures on quartz glass substrates are shown in Fig. 4. It can be seen from Fig. 4 that the films fired at 600 °C on quartz glass were pyrochlore phase, only several weak diffraction peaks of perovskite KTN being observed after heat treatment

at 750 °C. Although the structural transitions from pyrochlore to perovskite can be promoted at higher firing temperatures, many unidentified diffraction peaks appeared in the XRD pattern of the films fired at 900 °C. These unidentified diffraction peaks maybe due to the serious interdiffusion between these films and the substrates at such high temperature, which might be attributable to the alkali (potassium) reacting with SiO_2 in the substrates. On the other hand, differences in the XRD patterns of 750 and 900 °C annealed films suggested that the observed pyrochlores were of different compositions. Specifically, a broad peak at 15° 2θ was observed for 750 °C films and absent for 900 °C annealed films, whereas a broad peak at approximately 26° 2θ was observed for the 900 °C films and not the 750 °C.

Normally, the composition of the perovskite phase was found to be largely independent of the annealing temperature and close to the expected composition in all cases. In fact, XPS analysis of the perovskite phase in the 900 °C films on $SrTiO_3$ substrates was indistinguishable from that obtained for 750 °C perovskite, as the results for the KTN powders discussed above. However, on the other hand, the pyrochlore phases occurring at 750 and 900 °C were determined with differing potassium contents, being close to the expected concentration (i.e. of perovskite stoichiometry) in the 750 °C annealed sample, and potassium-deficient in the 900 °C annealed film. The presence of potassium-deficient pyrochlore observed in the sample annealed at 900 °C can be attributed to potassium loss from the film surface during annealing, as for lead-deficient pyrochlore in PZT films described in the literature [16, 17]. The important point in this case is that the transformation of such potassium-deficient pyrochlore to perovskite is not possible, owing to the stoichiometric restriction that the K: (Ta + Nb) ratio be close to unity [18].

KTN coatings on single-crystal silicon (1 1 1) which, because of atmospheric exposure, was coated with a thin layer of SiO_2 after heat treatment, have the same crystallization behaviour as those on quartz glass. Upon annealing to 600 °C, a pyrochlore phase was formed. Only a small portion of pyrochlore grain transformed into perovskite structure after annealing at 750 °C. The pyrochlore turned out to be the stable phase on silicon or quartz glass substrates and did not disappear or transform into perovskite completely, as was the case for KTN powder after higher temperature heat treatment.

Efforts to change the processing parameters in order to affect the structure and phase of the thin films that develop on silicon and quartz glass surfaces were conducted as follows. (1) To prevent the crystallization of pyrochlore below 700 °C, KTN films on silicon and on quartz glass were heated very rapidly in the 450–700 °C range or inserted cold into a preheated oven at 750 °C. XRD patterns of these films still showed pyrochlore phase as the major crystalline phase present. (2) A change in the amount of acetic acid added did not result in complete perovskite. (3) Because potassium loss was considered to be a possible contributor to pyrochlore formation, KTN solutions with 10 mol % excess potassium were prepared. Coatings made of these precursors on quartz glass or silicon (1 1 1) were heat treated to 750 °C. XRD patterns of the films again showed pyrochlore as the major phase and only small portion of perovskite phase present. (4) Heat treatment in oxygen resulted in lower temperatures of pyrochlore crystallization on films coated on quartz glass; the use of the gas, on the other hand, did not result in perovskite formation, even at 750 °C. (5) To prevent the interdiffusion of silicon with the films on surface of substrates, the KTN films were spin-coated on platinum-coated silicon (1 1 1). The XRD patterns of the films fired at 750 °C again indicated pyrochlore as the only phase present, as shown in Fig. 5.

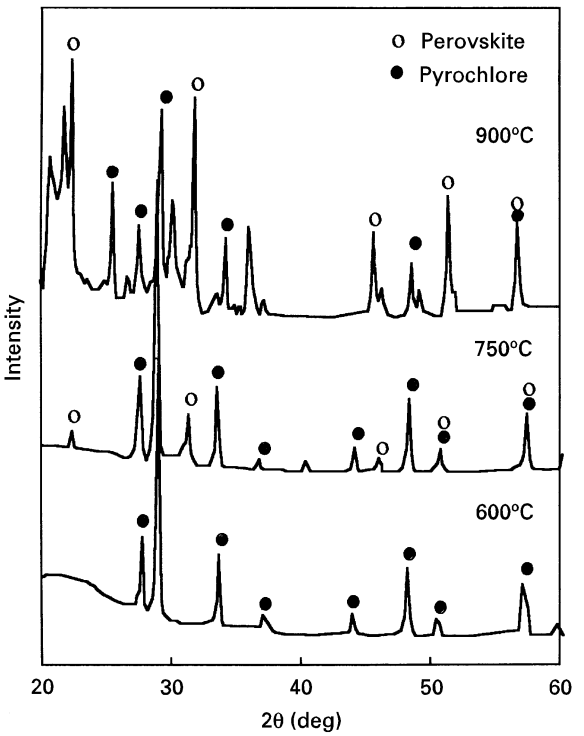

Figure 4 XRD patterns of KTN thin films on quartz glass fired at different temperatures.

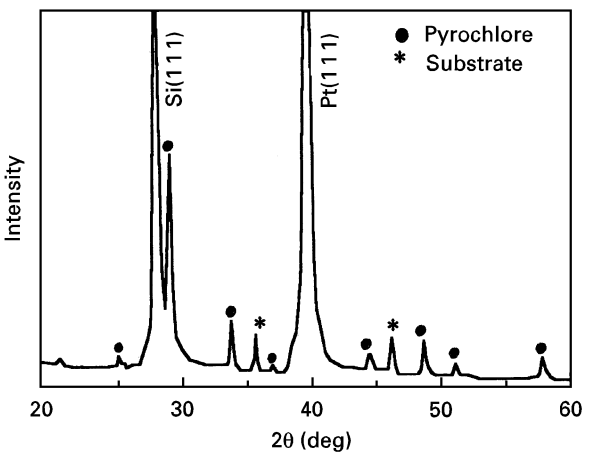

Figure 5 XRD pattern of KTN thin film on platinum coated silicon (1 1 1) fired at 750 °C.

The differences in the crystallization behaviour of KTN powder and of KTN thin film can originate from several factors. In the bulk form, hydrolysis is accomplished by exposing the KTN solution to atmospheric water. This results in a slow and gradual hydrolysis and polymerization. The result is a clear and monolithic wet gel. The resulting gelation process takes a few days and is usually accompanied by little or no shrinkage. If the resulting wet gel is exposed to the atmosphere, it loses the solvent and shrinks in three dimensions. Direct addition of water to the solution is accompanied by immediate precipitation which has been shown to result in non-stoichiometric KTN powders [19]. On the other hand, the collapse of a wet film that is only a few hundreds of nanometres in thickness to a solid gel occurs as the outcome of spinning it at high speeds. This is caused by rapid evaporation of the solvent and is many orders of magnitude faster than gel formation in the bulk KTN. These differences in structural developments of thin films and bulk gels have a great bearing on their subsequent characteristics. Furthermore, a film is confined to the substrate and tends to shrink only at 90° to it. The crystal structure of the substrate then has a great influence on the nucleation and crystal growth of the film.

3.2.2. YSZ, sapphire, $LaAlO_3$, and $SrTiO_3$ substrates

Five layers of 0.5 M KTN ($x = 0.35$) were deposited on YSZ (1 0 0), R-sapphire, $LaAlO_3$ (0 1 2), and $SrTiO_3$ (1 0 0) and (1 1 0) by spin-coating. All thin films heat treated to 450 °C were amorphous. Films heated to 600 °C for 1 h showed pyrochlore phase. When the films on YSZ (1 0 0) were heated to 750 °C for 1 h, they showed perovskite as the major phase and a pyrochlore content of about 35%. After the films were fired at 800 °C for 30 min, the pyrochlore changed to potassium-deficient pyrochlore because a broad peak at approximately 26° 2θ was observed in its XRD pattern (see Fig. 6). The transformation of such potassium-deficient pyrochlore to perovskite is not possible. Actually, the XRD pattern of the films fired at 900 °C is almost the same as that in Fig. 6. Therefore, it seems impossible that pyrochlore which existed in 750 °C heated films was transformed fully to pervoskite at higher temperatures.

Fig. 7a and b illustrate the XRD patterns of the films fired at 750 °C for 1 h on $LaAlO_3$ (0 1 2) and R-sapphire, respectively. The thin films consist principally of a perovskite (1 0 0) with preferred orientation with a small portion of pyrochlore. The XRD patterns of the films crystallized at 750 °C on $SrTiO_3$ (1 0 0) and (1 1 0) single-crystal substrates are shown in Fig. 8. These films showed complete crystallization and orientation along the (1 0 0) direction on (1 0 0) $SrTiO_3$ and (1 1 0) direction on (1 1 0) $SrTiO_3$, and X-ray diffraction gave no indication of any other phase. The reflection pattern of high-energy electron diffraction (RHEED) of the films on $SrTiO_3$ (1 0 0) was presented in the literature [20] and the diffraction spots were arranged in a regular array. It is certain from these

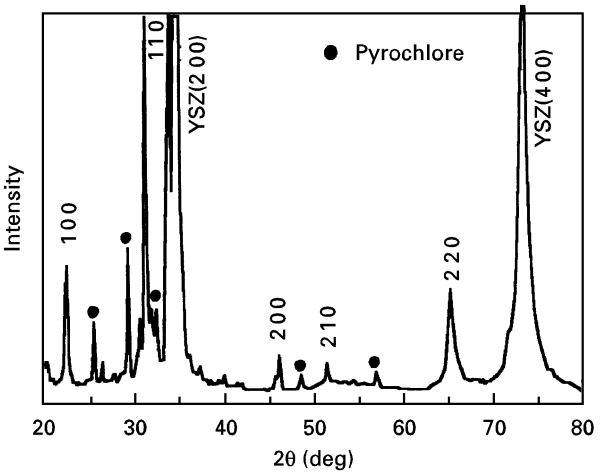

Figure 6 XRD pattern of KTN thin film on YSZ (1 0 0) fired at 800 °C.

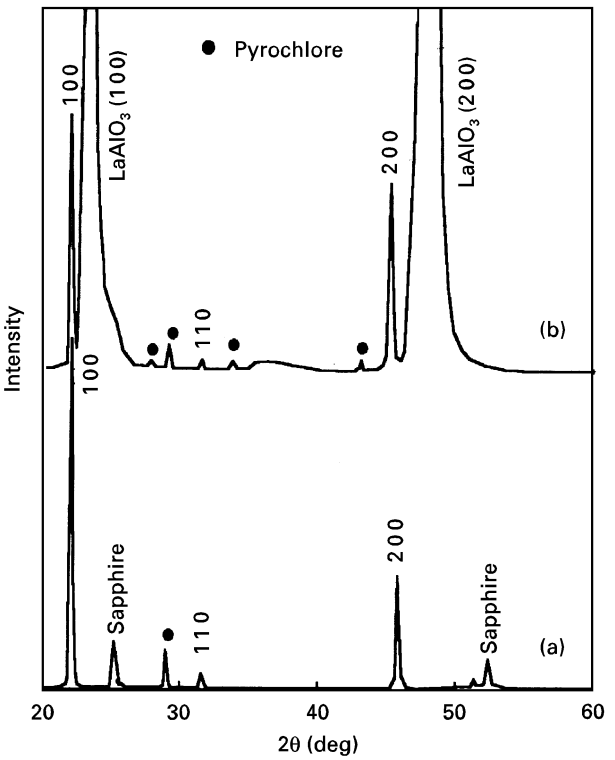

Figure 7 XRD patterns of KTN thin films on (a) R-sapphire and (b) $LaAlO_3$ (0 1 2), fired at 750 °C.

analyses that epitaxial KTN thin films were grown on $SrTiO_3$ substrates by the sol–gel method.

It can be seen from the above results that the crystal structure of the KTN thin films had a strong dependency on the crystal structure of the substrates, while other processing parameters played smaller roles. The influence of the substrate depends on both lattice matching and chemical bonding between the substrate and the film. Table II classifies the lattice matching of perovskite KTN films and various substrates. As can be seen in the table, $SrTiO_3$ has the same symmetry as perovskite KTN and the least d-spacing mismatch with perovskite KTN ($x = 0.35$) and is the best substrate for perovskite KTN formation and epitaxial growth.

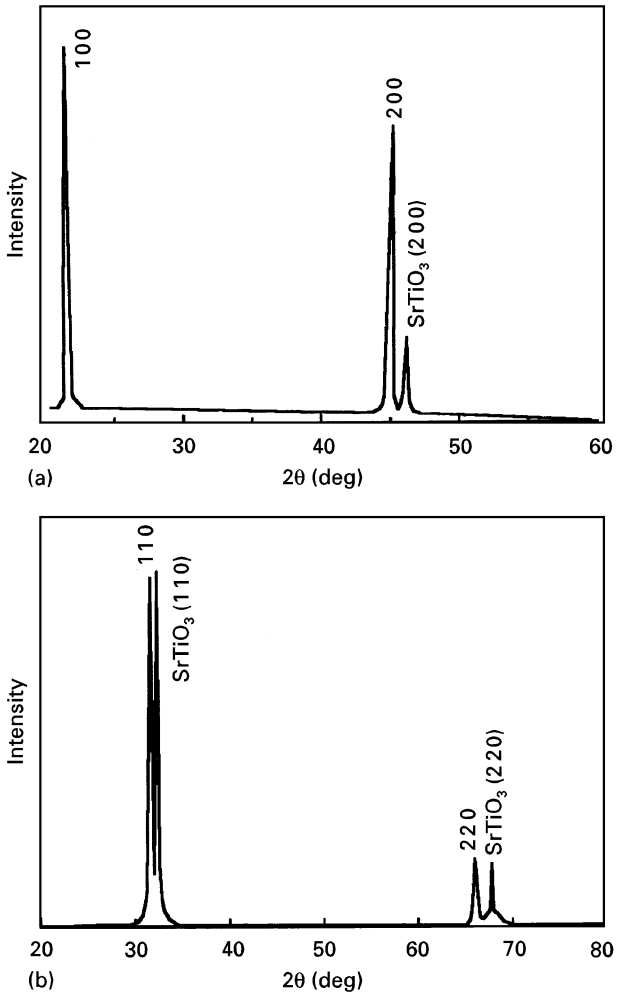

Figure 8 XRD patterns of KTN thin films on (a) $SrTiO_3$ (1 0 0) and (b) $SrTiO_3$ (1 1 0), fired at 750 °C.

Although sapphire has large differences of structure and lattice constant with perovskite KTN, the grains of perovskite KTN can possess an orientation matched with the R-sapphire surface due to a small O–O distance mismatch between the R-plane of sapphire and the (1 0 0) plane of KTN. We therefore obtained highly (1 0 0) preferentially oriented KTN films on R-sapphire substrates. This result is different from that reported by Hirano *et al.* [11]. In their experiments, only pyrochlore phase was observed on R-sapphire,

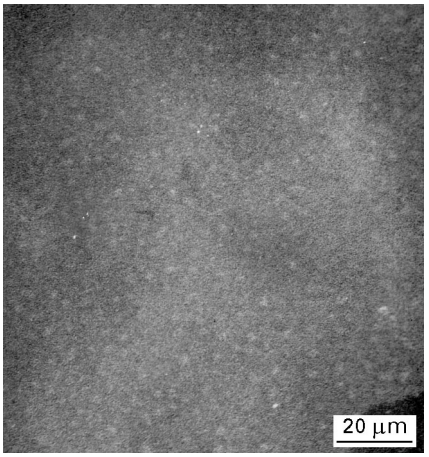

Figure 9 Scanning electron micrograph of the top surface of a KTN film fired at 750 °C for 1 h on $SrTiO_3$ (1 1 0).

even at 750 °C. The difference may be due to the different experimental details.

Although $LaAlO_3$ is of a trigonal symmetry and shows a pseudoperovskite structure at room temperature, it changes to cubic symmetry and perovskite structure above 560 °C (see Table II). Owing to the same crystal structure and small mismatch (5.0%) of the lattice constant during the annealing process at higher temperatures, the (1 0 0) oriented KTN thin films can grow on (0 1 2) $LaAlO_3$ substrates.

XPS and ICP measurements showed that the composition of the films on $SrTiO_3$ was nearly equal to the stoichiometry of the starting materials [21]. The usually observed deficiency of the volatile potassium in the deposited film was overcome. The scanning electron micrograph of the surface of the films formed on $SrTiO_3$ (1 1 0) at 750 °C for 1 h is shown in Fig. 9. The films appear crack- and pin hole-free with a smooth surface. The films were highly transparent. The electro-optical properties of the epitaxial films on $SrTiO_3$ (1 1 0) were initially investigated using a novel Faraday magneto-optic modulating system and the effective quadratic electro-optic coefficients were larger than 2.5×10^{-17} $m^2 V^{-2}$ at 632.8 nm, which will be reported in another paper.

TABLE II Lattice properties of materials in this work; oxygen lattice mismatch is calculated using oxygen distance value

	Crystal system	Crystal structure	Lattice constant (nm)	Oxygen distance value (nm)	Oxygen lattice mismatch with KTN (pero.) (%)
KTN ($x = 0.35$)	Cubic	Pyrochlore	1.0628	0.306	
		Perovskite	0.3993	0.282	
$SrTiO_3$	Cubic	Perovskite	0.3905	0.276	− 2.2
$LaAlO_3$	Trigonal	Pseudoperovskite	0.3792	0.268	− 4.9
(570 °C)	Cubic	Perovskite	0.3772	0.267	− 5.0
R-sapphire	Hexagonal	α-Al_2O_3	*a*: 0.4758	0.271	− 3.9
			c: 1.299		
YSZ	Cubic	Fluorite	0.5129	0.363	29.0
Pt	Cubic	fcc	0.3924		
Si	Cubic	Diamond	0.3138		
Quartz glass	Amorphous				

4. Conclusion

KTN precursors were prepared through sol–gel processing of metal alkoxides. KTN powders obtained by the gelation of KTN precursors in air exhibited a transient pyrochlore phase at 600 °C that transformed almost entirely into perovskite at 750 °C. In thin films, on the other hand, the pyrochlore phase which crystallized at low temperatures persisted at high temperatures on quartz glass, silicon, and platinum-coated silicon plates. The crystal structure of the KTN thin films had a strong dependency on the crystal structure of the substrates, whereas other processing parameters played smaller roles. Films deposited on YSZ (1 0 0) exhibited the perovskite structure as the major phase, with about 30% pyrochlore, even at 900 °C. Additionally, the films formed on $LaAlO_3$ (0 1 2) and R-sapphire consist principally of a perovskite (1 0 0) phase with a preferred orientation with a small portion of pyrochlore phase. Epitaxial KTN perovskite films were achieved on two orientations of $SrTiO_3$ single crystals and they were crack-free and transparent.

Acknowledgement

Thanks are extended to Mr Shiming Wang for his help in preparing the precursor solution. This work was supported by the Chinese National 863 Advanced Technology Project (715-03-02-01B).

References

1. S. TRIEBWASSER, *Phys. Rev.* 114 (1959) 63.
2. J. E. GEUSIC, S. K. KURTS, L. G. VAN UITERT and S. H. WEMPLE, *Appl. Phys. Lett.* **4** (1964) 141.
3. F. S. CHEN, J. E. GEUSIC, S. K. KURTS, L. G. VAN UITERT and S. H. WEMPLE, *J. Appl. Phys.* **37** (1966) 388.
4. O. M. STAFSUDD and M. Y. PINES, *J. Opt. Soc. Amer* **62** (1972) 1153.
5. A. J. FOX, *Appl. Opt.* **14** (1975) 343.
6. R. ORLOWSKI, L. A. BOATNER and E. KRÄTIG, *Opt. Commun.* **35** (1980) 45.
7. W. A. BONNER, E. F. DEARBORN and L. G. VAN UITERT, *Amer Ceram. Soc. Bull.* **44** (1965) 9.
8. A. L. GENTILE and F. H. ANDRES, *Mater. Res. Bull.* **2** (1967) 853.
9. A. REISMAN, S. TRIEBWASSER and F. HOLTZBEG, *J. Amer Chem. Soc.* **77** (1955) 4228.
10. P. E. DEBELY, P. E. GUNTER and H. AREND, *Amer Ceram. Soc. Bull.* **58** (1979) 606.
11. S. HIRANO, T. YOGO, K. KIKUTA, T. MORISHITA and Y. ITO, *J. Amer Ceram. Soc.* **75** (1992) 1701.
12. A. NAZERI and M. KAHN, *ibid.* **75** (1992) 2125.
13. C. J. LU, S. M. WANG, J. H. ZHAO, G. Y. HUANG, D. H. BAO and A. X. KUANG, *J. Inorg. Mater.* **8** (1993) 466 (in Chinese).
14. A. X. KUANG, C. J. LU, G. Y. HUANG and S. M. WANG, *J. Cryst. Growth* **149** (1995) 80.
15. Powder Diffraction File Alphabetical Index: Inorganic Phases (JCPDS, Swarthmore, PA, 1986).
16. I. M. REANEY, K. BOOKS, R. KLISSURSKA, C. PAWLACZYK and N. SETTER, *J. Amer Ceram. Soc.* **77** (1994) 1209.
17. B. A. TUTTLE, R. W. SCHWARTZ, D. H. DOUGHTY and J. A. VOIGT, in "Ferroelectric Thin Films", edited by E. R. Myers and A. I. Kingon (Materials Research Society, Pittsburgh, PA, 1990) pp.159–65.
18. M. A. SUBRAMANIAN, G. ARAVAMUDAN and G. V. SUBBA RAO, *Prog. Solid State Chem.* **15** (1983) 55.
19. E. T. WU, PhD thesis, University of California, Los Angeles, CA (1983).
20. D. H. BAO, A. X. KUANG, H. S. GU and S. M. WANG, *Chinese Sci. Bull.* **37** (1992) 1470.
21. C. J. LU, A. X. KUANG, G. Y. HUANG and S. M. WANG, *J. Mater. Sci.*, **31** (1996) 3081.

Received 4 December 1995
and accepted 10 February 1997